Spin and phase coherence measured by antilocalization in *n*-InSb thin films

R. L. Kallaher* and J. J. Heremans†
Department of Physics, Virginia Tech, Blacksburg, Virginia 24061, USA
(Received 22 September 2008; revised manuscript received 28 December 2008; published 25 February 2009)

The spin and phase coherence times of the itinerant electrons in *n*-InSb thin films were experimentally determined by analyzing the low-temperature magnetoresistance in antilocalization theory. The results indicate a very weak temperature dependence below 10 K for the spin coherence time. The dependence of the spin coherence time on carrier density demonstrates that the Elliott-Yafet mechanism is predominantly responsible for electron-spin relaxation in *n*-type InSb at low temperatures. The phase coherence time follows an inverse temperature dependence, in accordance with the electron-electron Nyquist dephasing mechanism.

DOI: 10.1103/PhysRevB.79.075322 PACS number(s): 73.61.Ey, 73.20.Fz, 72.25.Rb

I. INTRODUCTION

Distinct electrical transport properties of value for magnetic field sensors[1] and high-speed transistors,[2] together with strong spin-orbit (SO) interactions,[3] render the narrow gap semiconductor InSb and its heterostructures promising candidates for spintronics studies.[4] An analysis of the mechanisms of spin and phase decoherence in InSb thin films forms a necessary part of these studies. Two SO scattering mechanisms determine spin decoherence in *n*-type InSb thin films:[5–7] the D'yakonov-Perel (DP) mechanism[8] and the Elliott-Yafet (EY) mechanism.[9] Spin decoherence via the DP mechanism is a consequence of electron-spin precession in the effective magnetic field generated by SO interactions. Separately, under SO interactions opposing spin states admix in an itinerant electron's Bloch wave function,[9] and momentum scattering then leads to spin decoherence via the EY mechanism. At a given temperature T and given mobility μ, the relative importance of the two mechanisms depends on the semiconductor band gap, E_G, and the SO splitting of its valence bands, Δ. The EY mechanism can gain prominence in materials with small E_G and large Δ, such as InSb.[5,6] The DP mechanism dominates spin decoherence in many other *n*-type III-V materials and heterostructures, especially at higher T and higher μ.[10,11] Evidence suggests that a transition occurs between the DP and EY mechanisms in InSb films from DP at high T and higher μ to EY at low T and lower μ.[7,12,13]

In order to obtain values for the spin coherence time τ_{SO} and the phase coherence time τ_ϕ and to determine decoherence mechanisms in InSb, we performed detailed measurements over T of the low-field magnetoresistance on thin films of *n*-InSb at different electron densities (n) and electron μ. Quantum interference between backscattered time-reversed trajectories leads to a correction to the classically predicted resistance value.[14,15] Under weak SO interactions, constructive interference causes an increase in the resistance known as weak localization (WL).[14–16] Under strong SO interactions, destructive interference causes a decrease in resistance known as antilocalization (AL).[14,15,17–20] An external magnetic field H destroys time-reversal symmetry, resulting in a magnetoresistance carrying quantitative information about phase and spin scattering.[15] The magnetoresistance has become a valuable tool to experimentally study τ_ϕ (Refs. 16 and 20–22) and τ_{SO} (Refs. 19–23) in semiconducting systems. Previous work on doped *n*-type bulk InSb crystals ($n < \sim 10^{21}$ m^{-3}) has shown distinct WL (Ref. 24) but no AL. A recent observation of AL in Pb-doped, low μ, polycrystalline InSb films ($n > 10^{22}$ m^{-3}) attributes strong SO scattering to Pb doping,[25] while a study in Sn-doped InSb films ($n \approx 7 \times 10^{22}$ m^{-3}) concludes that the DP mechanism dominates.[26] The present work systematically examines AL phenomena in InSb films with distinctly different n and μ to present a coherent study of AL in high-quality InSb thin films.

II. EXPERIMENT

The magnetoresistances of three InSb films were measured in a perpendicularly applied H via standard four-contact low-frequency lock-in techniques. Each film, grown by metal-organic chemical-vapor deposition (MOCVD) on semi-insulating GaAs ⟨100⟩ substrate, is composed of three InSb layers: first, a 0.15–0.2 μm buffer layer directly on the GaAs substrate; second, the high μ Te-doped active layer; and on top, a low μ heavily doped 0.05 μm cap layer to facilitate Ohmic contacts. Structural details of the InSb films are listed in Table I and elsewhere.[27] The films differ mostly in the active layer by the active-layer doping level N_D and active-layer thickness t, and indeed the active-layer parameters dominate the measured transport properties. Measurements of μ vs etch depth on similar films demonstrate that both the buffer layer and cap layer have a significantly lower

TABLE I. The layer structure for the different InSb film types: buffer layer thickness (t_{buffer}) and Te doping ($N_{D,buffer}$, UD = undoped), active-layer thickness (t) and Te doping (N_D), and cap-layer thickness (t_{cap}) and Te doping ($N_{D,cap}$).

	A	B	C
t_{buffer} (μm)	0.2	0.15	0.2
$N_{D,buffer}$ (10^{22} m^{-3})	UD	UD	4
t(active) (μm)	1.3	0.6	1.3
N_D(active) (10^{22} m^{-3})	2	3	10
t_{cap} (μm)	0.05	0.05	0.05
$N_{D,cap}$ (10^{22} m^{-3})	15	15	30

TABLE II. The active-layer transport properties for the different InSb film types: electron density (n), mobility (μ), Fermi energy (E_F), and wavelength (λ_F) at $T=0.4$ K.

	A	B	C
n (10^{22} m^{-3})	0.6–0.7	2.8–3.1	8.8–9.0
μ (m^2/Vs)	4.0–4.4	3.4–3.5	4.4–4.5
E_F (meV)	8.3–9.2	22.0–23.4	43.5–44.1
λ_F (μm)	0.11	0.07	0.05

average μ than the active layer.[28] The buffer layer mitigates the effect of threading dislocations arising from the 14% lattice mismatch at the GaAs/InSb interface. The threading dislocations depress the mobility of the interface layer and act as n-type dopants. To further increase the resistance of the buffer layer, either no or low intentional Te doping is employed in this layer. In addition, depletion of carriers from the surface of the semiconducting film further increases the cap-layer resistance relative to the active-layer resistance. The data have thus been analyzed assuming a dominant contribution to the magnetoresistance from the active layer only, neglecting contributions from the buffer and cap layers. This assumption is supported by a multilayer in-plane magnetotransport analysis[29] which suggests that the active layer conducts ~95% of the overall current.

Hall effect and resistivity measurements were performed in order to characterize the active layers at low T. Table II summarizes the low T transport properties. Experimental values for n and μ correspond to the active-layer properties, confirming that little or no current is conducted by the buffer and cap layers. Sample type A corresponds to a lightly doped thick active layer, yielding high μ at low n.[1] Sample type B features a moderately doped thin active layer, resulting in lower μ at intermediate n. Sample type C corresponds to a highly doped thick active layer with high μ and high n. The dependence of μ on T is nonmonotonic[27] and typically exhibits a maximum in μ (at $T\approx 200$ K for sample A, $T\approx 300$ K for sample B, and $T\approx 80$ K for sample C), indicating a competition between phonon scattering and screened n-dependent Coulombic ionized dopant scattering as μ-limiting scattering mechanisms.[30] Phonon scattering dominates at higher T, whereas Coulombic scattering dominates at low T where WL and AL phenomena can be observed. The level of Coulombic scattering in the active layer results from a balance between increased ionized dopant concentrations at higher N_D on one hand and increased screening due to the higher n at higher N_D on the other. This trade off has been used previously to optimize InSb layers for magnetic sensor applications.[27] In sample B with thinner buffer and active layers, threading dislocations reaching into the active layer may also contribute to a lower μ and higher n. Threading dislocations act as n-type dopants and likewise result in Coulombic scattering. In short, at low T, ionized dopants and dislocations in the active layers determine n and limit μ through Coulombic mechanisms. Phenomena such as surface scattering are not believed to play a discernible role in the active layers.

III. RESULTS AND DISCUSSION

Figure 1 contains examples of the magnetoresistance in the films. To account for contributions from the Hall effect as well as electronic drifts, the component of the data antisymmetric in H has been subtracted from the data. Clear AL phenomena occur in all three films as evidenced by the sharp positive magnetoresistance around $H=0$ crossing over to negative magnetoresistance at higher H. In the range of τ_ϕ and τ_{SO} of the films, τ_{SO} largely determines the separation in H between the resistance maxima, with a lower τ_{SO} leading to broader curves. The depth of the resistance minimum increases with the ratio τ_ϕ/τ_{SO}. Qualitatively, the T dependence of the positive magnetoresistance is most pronounced at the lowest dopant density (A), where the resistance minimum at $H=0$ due to AL was not observable for $T>3$ K. The AL effect remains observable for $T>7$ K at heavier doping (B and C), reflecting a higher ratio τ_ϕ/τ_{SO}. In the more heavily doped samples (B and C), however, the spin decoherence is more pronounced as evidenced by the relative broadness of the curves, consistent with increasing SO interaction and SO scattering rate at increasing n and increasing Fermi energy, E_F.[5,6,31] The fact that the observed AL phenomena are sensitive to the active layer n and are not correlated with its thickness confirms that the magnetoresistance predominantly probes the active layer and quantifies the spin and phase decoherence in this layer.

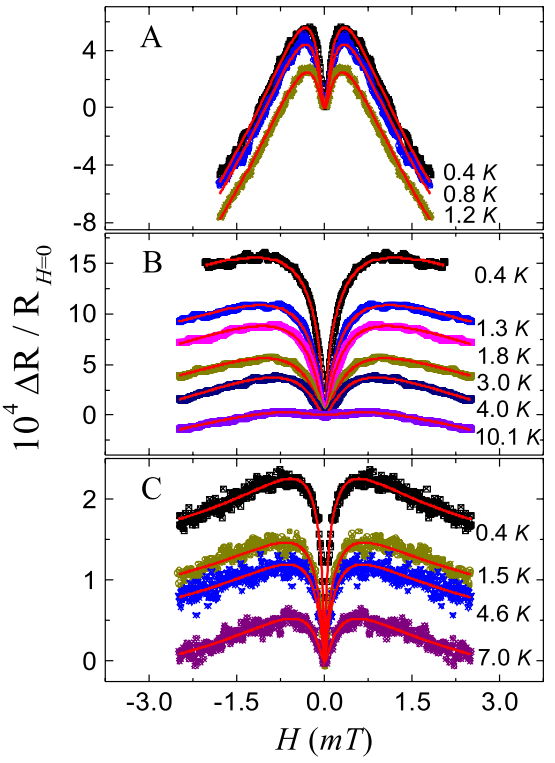

FIG. 1. (Color online) Measured low H magnetoresistance at variable T, along with the fits to Eq. (1), for the InSb films A, B, and C.

In all the films the mobility mean-free path and the Fermi wavelength, λ_F, are shorter than the active-layer thickness, t. Therefore, the films are considered kinematically three dimensional, and the Fermi velocity v_F and the diffusion constant D are evaluated three dimensionally ($D=\frac{1}{3}v_F^2\tau_p$, where τ_p is the momentum scattering time). However, the WL and

AL quantum corrections to the conductivity are phase coherence phenomena, and hence the dimensionality used to calculate the WL and AL corrections depends on the relative magnitudes of the phase coherence length, $L_\phi=\sqrt{D\tau_\phi}$, and t.[15,32,33] When $L_\phi>t$, phase coherence phenomena—such as the WL and AL corrections to resistivity—follow two-dimensional behavior even when the film is kinematically three dimensional. The low T values for τ_ϕ, as obtained from fitting the data to AL theory, are self-consistently found to yield $L_\phi>t$ for all T at which AL was observed. Hence, the magnetoresistance was fitted to a two-dimensional localization theory developed by Hikami, Larkin, and Nagaoka (HLN).[17] Films that are kinematically three dimensional yet two dimensional regarding phase coherence phenomena are commonly encountered in studies on metals.[15,32,33] In the HLN theory[17] we also neglect magnetic scattering leading to spin flip,[34] since no magnetic impurities are explicitly present in the InSb films. AL analysis cannot provide independent quantification of the inelastic-scattering limiting τ_ϕ and of magnetic spin-flip scattering.[34–37] In the absence of independent knowledge allowing a quantification of magnetic spin-flip scattering, this mechanism is presumed negligible. For isotropic SO scattering in perpendicular H the correction to the resistivity is then[15,17,32]

$$\Delta\rho/[\rho^2(H=0)] \approx -\Delta\sigma = \frac{e^2}{2\pi^2\hbar}\left[\Psi\left(\frac{1}{2}+\frac{H_{\rm tr}}{H}\right) + \frac{1}{2}\Psi\left(\frac{1}{2}+\frac{H_\phi}{H}\right) - \frac{3}{2}\Psi\left(\frac{1}{2}+\frac{H_\phi}{H}+\frac{4}{3}\frac{H_{\rm SO}}{H}\right)\right], \quad (1)$$

where Ψ is the digamma function and $H_{\rm tr}=\hbar/(4eD\tau_p)$, $H_\phi=\hbar/(4eD\tau_\phi)$, and $H_{\rm SO}=\hbar/(4eD\tau_{\rm SO})$.

With τ_p and D independently determined from Hall measurements and from the resistivity at $H=0$, a least-squares fit to Eq. (1) was employed to determine both $\tau_{\rm SO}$ and τ_ϕ at each T. Figure 2 contains the resulting values. Within experimental errors all samples show a $\tau_{\rm SO}$ independent of T for $0.4<T<10$ K. The pronounced T dependence of τ_ϕ is depicted in the inset of Fig. 2 and will be discussed below. Thus the T dependence in Fig. 1 is dominated by the behavior of τ_ϕ through the ratio $\tau_\phi/\tau_{\rm SO}$, as mentioned above. In particular, in sample A the long $\tau_{\rm SO}$ lowers the ratio $\tau_\phi/\tau_{\rm SO}$ and restricts the range of T over which AL could be observed.

The extracted values of $\tau_{\rm SO}$ exhibit a strong dependence on n, with $\tau_{\rm SO}$ varying from ~6 ps in sample C (highest n) to ~73 ps in sample A (lowest n). Because of the high electron μ in InSb (Table II), the spin coherence lengths $L_{\rm SO}=\sqrt{D\tau_{\rm SO}}$ can be considerable in InSb films; values of $L_{\rm SO}$ are illustrated in Fig. 2. Our experiments indicate an $L_{\rm SO}$ as long as 1.5 μm. Even at high n, we find $L_{\rm SO}>1$ μm. Such length scales are readily achieved with modern microfabrication techniques, allowing a spin-coherent regime to be accessed.[4]

The EY and DP mechanisms differ in their dependences on E_F and τ_p,[5–7,13]

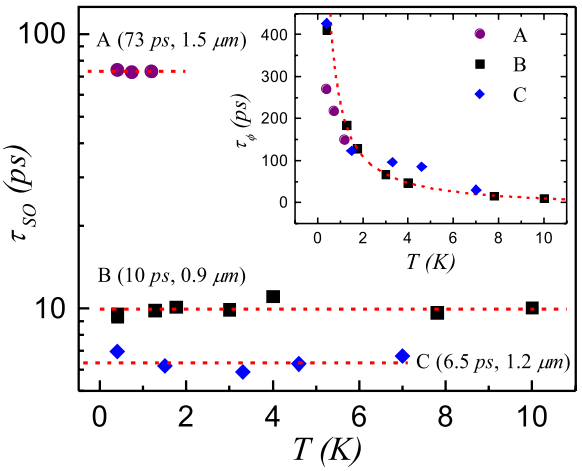

FIG. 2. (Color online) Main panel: the spin coherence times $\tau_{\rm SO}$ vs T, obtained from the fits of Eq. (1) to the data in Fig. 1. The dashed horizontal lines indicate average values of $\tau_{\rm SO}$, also in parentheses with the spin coherence length. Inset: the extracted phase coherence times τ_ϕ vs T. The dashed line indicates a fit to a $1/T$ dependence.

$$\frac{1}{\tau_{\rm SO}^{\rm EY}}=\frac{\alpha_{\rm EY}}{\tau_p}\left(\frac{E_F}{E_G}\right)^2, \quad \frac{1}{\tau_{\rm SO}^{\rm DP}}=\alpha_{\rm DP}\tau_p\left(\frac{E_F^3}{\hbar^2E_G}\right), \quad (2)$$

where $\alpha_{\rm EY,DP}$ are material constants. Equation (2) holds for degenerate semiconductors at low T.[5,6,13,38] Calculation of $E_F(T)$ indicates that the degenerate regime indeed applies to the present samples. In Eq. (2) τ_p provides a measure of the electron-scattering time with a different effect in EY and DP regimes. In the DP regime frequent scattering events interrupt the spin precession, resulting in small average spin precession angles and a suppression of dephasing among precession angles (motional narrowing), and hence to $\tau_{\rm SO}\sim 1/\tau_p$. In the EY regime the scattering events, assumed more sparse, do not result in motional narrowing and instead spin dephases through SO coupling at the orbital scattering event itself, leading to $\tau_{\rm SO}\sim\tau_p$.[5–7] Thus, the EY mechanism is weaker in materials with high μ. Nonetheless, it has been shown that even in ballistic systems AL is sensitive to spin relaxation via the EY mechanism,[39] and in the narrow gap semiconductors at low T, the EY mechanism is thought to dominate.[6,7,39]

Figure 3 depicts the dependence of $1/\tau_{\rm SO}$ on E_F, determined using the measured n and accounting for nonparabolicity in the InSb band structure.[40] In order to accommodate the different μ in each film, the measured $1/\tau_{\rm SO}$ has been multiplied by τ_p. Because $1/\tau_{\rm SO}\sim E_F^\nu$ for both EY ($\nu=2$) and DP ($\nu=3$) mechanisms, a logarithmic plot of $1/\tau_{\rm SO}$ vs E_F indicates which mechanism dominates spin decoherence. A fit to the data in Fig. 3 yields $\nu=2.06$, strongly indicating that EY is the dominant spin decoherence mechanism in the InSb films. This result agrees with electron-spin-resonance linewidths in n-type ($n<10^{22}$ m^{-3}) bulk InSb.[13]

For Coulombic scattering in degenerate semiconductors, $\alpha_{\rm EY}$ is theoretically predicted as[5,13]

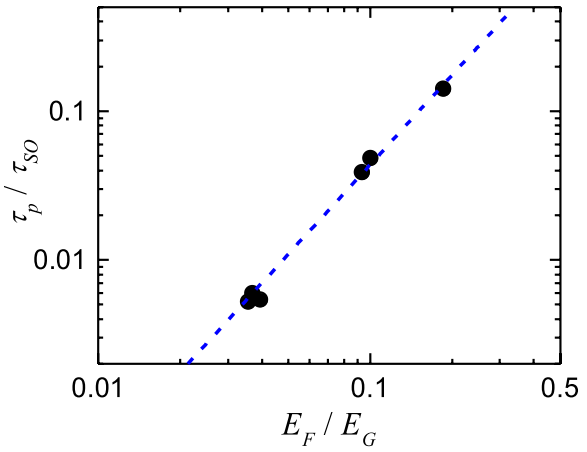

FIG. 3. (Color online) Logarithmic plot of the average spin decoherence rate, $1/\tau_{SO}$ (normalized to $1/\tau_p$) (see text). The dashed line denotes the functional dependence $1/\tau_{SO} \sim (E_F/E_G)^2$ as predicted from the EY spin decoherence theory.

$$\alpha_{EY} = \frac{32}{27}\gamma^2\left(\frac{1-\gamma/2}{1-\gamma/3}\right)^2, \tag{3}$$

where $\gamma=\Delta/(\Delta+E_G)$ [$\Delta=810$ meV and $E_G=236$ meV in InSb at low T (Ref. 3)]. The measured rate $1/\tau_{SO}$ is, however, a factor of ~ 9 higher than predicted from Eq. (3) when using τ_p as the characteristic scattering time scale. This fact suggests that scattering events with only a small effect on μ, such as small-angle or electron-electron scattering, may have, in contrast, a large effect on spin decoherence.[41] In the calculation of $1/\tau_p$, the scattering angle θ weighs scattering probabilities by a factor of $1-\cos(\theta)$, whereas other weight factors are appropriate for $1/\tau_{SO}$. An analogy can be drawn with two-dimensional electron systems dominated by the DP mechanism, where accurate prediction of τ_{SO} requires a proper account of the symmetry of the scattering mechanisms.[10,11,19,41] For bulk InSb with spin relaxation resulting from the cubic Dresselhaus SO coupling term, the use of τ_3, defined by

$$\frac{1}{\tau_3} = \int_{-1}^{1} W(\theta)\{1 - P_3[\cos(\theta)]\} d\cos(\theta), \tag{4}$$

rather than τ_p is appropriate for a calculation of $1/\tau_{SO}$.[11] Here $W(\theta)$ denotes the θ-dependent scattering probability and P_3 denotes the third Legendre polynomial. For Coulombic scattering and in the limit of weak screening in bulk semiconductors, we have calculated $\tau_3/\tau_p \approx 1/6$. The observed independence of τ_{SO} on T suggests that for $0.4 < T < 10$ K Coulombic scattering from ionized species dominates. Furthermore, weak screening applies to the InSb samples in this study, where the small effective mass leads to a Thomas-Fermi wave vector, $q_{TF} \approx 5-6\times 10^7$ m^{-1}, a factor of ~ 2 smaller than the Fermi wave vector. Our value $\tau_3/\tau_p \approx 1/6$ compares to $\sim 1/9$ found for two-dimensional electron systems.[10,11,19] Thus, we expect that the use of τ_p underestimates the spin decoherence rate, whereas the use of τ_3 brings the experimental values within a factor 1.5 of theoretical predictions. The presence of an enhanced spin decoherence rate in the InSb films forms a possible reason why the predicted transition[7] from the EY to DP mechanism as a function of T was not experimentally observed.

Equation (1) (Ref. 17) assumes a dominant EY mechanism and is valid in the diffusive limit. HLN theory was favored here because it experimentally provided a better fit to the magnetoresistance data than theories[18] intended for systems beyond the diffusive limit. However, a similar functional dependence of the spin decoherence rate on E_F is recovered when either an AL theory that assumes a dominant DP mechanism[14] or a theory that is valid beyond the diffusive limit[18] is applied. Thus, the conclusion that the EY mechanism dominates the SO scattering is consistent, regardless of the AL theory. In addition for all AL theories tried, the experimental values for τ_{SO} are significantly lower than predicted by theory using τ_p.[13]

In the range of T where AL is experimentally accessible, both samples B and C yield $\tau_\phi \sim 1/T$. The inset of Fig. 2 depicts the T dependence of τ_ϕ and the $1/T$ fit for sample B. An excellent fit is obtained apart from saturation of τ_ϕ observed at $T=0.4$ K. Saturation of τ_ϕ at $T<1$ K is a feature common to many systems, indicating that additional phase-breaking mechanisms limit τ_ϕ.[15,21,42] Electron-electron scattering in a Fermi-liquid model leads to the Nyquist phase decoherence rate[21,43,44] as adapted from Ref. 43 for a thin film of thickness t,

$$\frac{1}{\tau_\phi} = \frac{k_B T}{2\pi\hbar^2 D g(E_F) t} \ln[\pi\hbar D g(E_F) t], \tag{5}$$

where $g(E_F)$ denotes the (nonparabolic) density of states at E_F. The Nyquist rate follows the observed dependence $\tau_\phi \sim 1/T$ and is valid if the thermal length $L_T = \sqrt{\hbar D/k_B T}$ is not much smaller than t, a condition fulfilled in our samples. Sample B experimentally yields $\tau_\phi = (254\ \text{Kps})/T$, whereas the Nyquist expression results in $\tau_\phi = (570\ \text{Kps})/T$. Theory thus predicts a phase decoherence rate approximately twice smaller than observed. The discrepancy is deemed acceptable, since discrepancies in the literature[21] can amount to orders of magnitude, with the experimental phase decoherence rates exceeding theoretical predictions. We note that the experimental phase decoherence rate in Sample C does indeed exceed the theoretical Nyquist rate by 1 order of magnitude, even as $\tau_\phi \sim 1/T$ is closely obeyed for this sample as well.

IV. CONCLUSIONS

In conclusion, the dependence on E_F of the low-T spin decoherence rate as extracted from AL demonstrates that the EY mechanism dominates spin decoherence in high-quality InSb Te-doped thin films for $T<10$ K. The observation $1/\tau_{SO} \sim E_F^2$ indicates that at low T long τ_{SO} can exist in high-quality InSb with E_F just above the conduction band edge. We have determined a spin coherence length as long as 1.5 μm in an InSb film with $E_F \approx 9$ meV. The experimental spin coherence times are shorter than predicted by the EY model if the momentum scattering time τ_p is assumed as a

relevant scattering time. Substituting a scattering time appropriately weighed for spin decoherence due to the cubic Dresselhaus SO coupling under Coulombic scattering brings the EY model in closer agreement with the experimental data. Phase coherence times experimentally follow $\tau_\phi \sim 1/T$. Acceptable agreement with the Nyquist electron-electron scattering mechanism in thin films is concluded, although experimental phase coherence times remain shorter than the Nyquist prediction.

ACKNOWLEDGMENTS

This work was supported by NSF through Grant No. DMR-0618235. Work partially performed while R.L.K. was supported by MARTECH, Florida State University

*kallaher@vt.edu
†heremans@vt.edu

[1] S. A. Solin, T. Thio, D. R. Hines, and J. J. Heremans, Science **289**, 1530 (2000).
[2] T. Ashley, A. B. Dean, C. T. Elliot, G. J. Pryce, A. D. Johnson, and H. Willis, Appl. Phys. Lett. **66**, 481 (1995).
[3] O. Madelung, *Semiconductors: Data Handbook*, 3rd ed. (Springer, Berlin, 2004).
[4] H. Chen, J. J. Heremans, J. A. Peters, A. O. Govorov, N. Goel, S. J. Chung, and M. B. Santos, Appl. Phys. Lett. **86**, 032113 (2005).
[5] G. E. Pikus and A. N. Titkov, in *Optical Orientation*, edited by F. Meier and B. P. Zakharchenya (North-Holland, Amsterdam, 1984).
[6] I. Zutic, J. Fabian, and S. Das Sarma, Rev. Mod. Phys. **76**, 323 (2004).
[7] P. H. Song and K. W. Kim, Phys. Rev. B **66**, 035207 (2002).
[8] M. I. D'yakonov and V. I. Perel', Sov. Phys. JETP **33**, 1053 (1971).
[9] R. J. Elliott, Phys. Rev. **96**, 266 (1954); Y. Yafet, in *Solid State Physics*, edited by F. Seitz and D. Turnbull (Academic, New York, 1963), Vol. 14.
[10] J. Kainz, U. Rössler, and R. Winkler, Phys. Rev. B **70**, 195322 (2004).
[11] W. H. Lau, J. T. Olesberg, and M. E. Flatté, Phys. Rev. B **64**, 161301(R) (2001).
[12] K. L. Litvinenko, L. Nikzad, J. Allam, B. N. Murdin, C. R. Pidgeon, J. J. Harris, T. Zhang, and L. F. Cohen, J. Appl. Phys. **101**, 083105 (2007).
[13] J. N. Chazalviel, Phys. Rev. B **11**, 1555 (1975).
[14] B. L. Altshuler, A. G. Aronov, A. I. Larkin, and D. E. Khmel'nitskii, Sov. Phys. JETP **54**, 411 (1981).
[15] G. Bergmann, Phys. Rep. **107**, 1 (1984).
[16] S. McPhail, C. E. Yasin, A. R. Hamilton, M. Y. Simmons, E. H. Linfield, M. Pepper, and D. A. Ritchie, Phys. Rev. B **70**, 245311 (2004).
[17] S. Hikami, A. I. Larkin, and Y. Nagaoka, Prog. Theor. Phys. **63**, 707 (1980).
[18] A. Zduniak, M. I. Dyakonov, and W. Knap, Phys. Rev. B **56**, 1996 (1997).
[19] W. Knap, C. Skierbiszewski, A. Zduniak, E. Litwin-Staszewska, D. Bertho, F. Kobbi, J. L. Robert, G. E. Pikus, F. G. Pikus, S. V. Iordanskii, V. Mosser, K. Zekentes, and Y. B. Lyanda-Geller, Phys. Rev. B **53**, 3912 (1996).
[20] J. B. Miller, D. M. Zumbühl, C. M. Marcus, Y. B. Lyanda-Geller, D. Goldhaber-Gordon, K. Campman, and A. C. Gossard, Phys. Rev. Lett. **90**, 076807 (2003).
[21] S. A. Studenikin, P. T. Coleridge, N. Ahmed, P. J. Poole, and A. Sachrajda, Phys. Rev. B **68**, 035317 (2003).
[22] D. D. Bykanov, A. M. Kreshcuk, S. V. Novikov, T. A. Polyanskaya, and I. G. Savel'ev, Semiconductors **32**, 985 (1998).
[23] T. Koga, J. Nitta, T. Akazaki, and H. Takayanagi, Phys. Rev. Lett. **89**, 046801 (2002).
[24] R. C. Dynes, T. H. Geballe, G. W. Hull, Jr., and J. P. Garno, Phys. Rev. B **27**, 5188 (1983); R. G. Mani, L. Ghenim, and J. B. Choi, *ibid.* **43**, 12630 (1991).
[25] M. Oszwaldowski, T. Berus, and V. K. Dugaev, Phys. Rev. B **65**, 235418 (2002).
[26] S. Ishida, K. Takeda, A. Okamoto, and I. Shibasaki, Physica E (Amsterdam) **20**, 211 (2004).
[27] M. W. Pelczynski, J. J. Heremans, and S. Schwed, Mater. Res. Soc. Symp. Proc. **607**, 65 (2000).
[28] D. L. Partin, M. Pelczynski, P. Cooke, L. Green, J. Heremans, and C. M. Thrush, J. Cryst. Growth **195**, 378 (1998).
[29] R. L. Petritz, Phys. Rev. **110**, 1254 (1958).
[30] W. Zawadzki and W. Szymanska, J. Phys. Chem. Solids **32**, 1151 (1971).
[31] G. Dresselhaus, Phys. Rev. **100**, 580 (1955).
[32] S. Kobayashi and F. Komori, Prog. Theor. Phys. Suppl. **84**, 224 (1985).
[33] Z. Ovadyahu and Y. Imry, Phys. Rev. B **24**, 7439 (1981).
[34] C. Van Haesendonck, J. Vranken, and Y. Bruynseraede, Phys. Rev. Lett. **58**, 1968 (1987).
[35] W. Wei and G. Bergmann, Phys. Rev. B **37**, 5990 (1988).
[36] H. Beckmann and G. Bergmann, Phys. Rev. B **54**, 368 (1996).
[37] R. P. Peters, G. Bergmann, and R. M. Mueller, Phys. Rev. Lett. **60**, 1093 (1988).
[38] K. L. Litvinenko, B. N. Murdin, J. Allam, C. R. Pidgeon, T. Zhang, J. J. Harris, L. F. Cohen, D. A. Eustace, and D. W. McComb, Phys. Rev. B **74**, 075331 (2006).
[39] K. S. Romanov and N. S. Averkiev, JETP **101**, 699 (2005).
[40] W. Zawadzki and W. Szymanska, Phys. Status Solidi B **45**, 415 (1971).
[41] M. A. Brand, A. Malinowski, O. Z. Karimov, P. A. Marsden, R. T. Harley, A. J. Shields, D. Sanvitto, D. A. Ritchie, and M. Y. Simmons, Phys. Rev. Lett. **89**, 236601 (2002).
[42] P. Mohanty, E. M. Q. Jariwala, and R. A. Webb, Phys. Rev. Lett. **78**, 3366 (1997).
[43] B. L. Altshuler, A. G. Aronov, and D. E. Khmelnitsky, J. Phys. C **15**, 7367 (1982).
[44] A. G. Huibers, M. Switkes, C. M. Marcus, K. Campman, and A. C. Gossard, Phys. Rev. Lett. **81**, 200 (1998).